

# The Low-Noise Potential of Distributed Propulsion on a Catamaran Aircraft

Joe W. Posey\*

*NASA Langley Research Center*

A.F. Tinetti†

*NCI Information Systems, Inc.*

and

M.H. Dunn‡

*National Institute of Aerospace*

The noise shielding potential of an inboard-wing catamaran aircraft when coupled with distributed propulsion is examined. Here, only low-frequency jet noise from mid-wing-mounted engines is considered. Because low frequencies are the most difficult to shield, these calculations put a lower bound on the potential shielding benefit. In this proof-of-concept study, simple physical models are used to describe the 3-D scattering of jet noise by conceptualized catamaran aircraft. The Fast Scattering Code is used to predict noise levels on and about the aircraft. Shielding results are presented for several catamaran type geometries and simple noise source configurations representative of distributed propulsion radiation. Computational analyses are presented that demonstrate the shielding benefits of distributed propulsion and of increasing the width of the inboard wing. Also, sample calculations using the FSC are presented that demonstrate additional noise reduction on the aircraft fuselage by the use of acoustic liners on the inboard wing trailing edge. A full conceptual aircraft design would have to be analyzed over a complete mission to more accurately quantify community noise levels and aircraft performance, but the present shielding calculations show that a large acoustic benefit could be achieved by combining distributed propulsion and liner technology with a twin-fuselage planform.

## Nomenclature

$p'$  = acoustic pressure,

$\vec{v}'$  = acoustic velocity,

$\rho_0$  = local density,

$c_0$  = local speed of sound,

$\vec{M}_0$  = local Mach number vector,

$k_0 = \frac{\omega}{c_0}$  = local wave number,

$\omega$  = excitation frequency,

$S$  = scattering surface boundary,

$S^+$  = scattering surface exterior,

$A = 1/Z$  = acoustic admittance,

$Z$  = complex normal impedance,

$\hat{n}$  = unit outward surface normal.

---

\* Senior Research Engineer for Acoustics, Research and Technology Directorate, Associate Fellow.

† Research Scientist, Senior Member.

‡ Consultant, Senior Member.

## I. □ Introduction

Both NASA and the European Union (EU) have advanced the vision of keeping objectionable aircraft noise within airport boundaries. [In keynote addresses at the 2001 AIAA/CEAS Aeroacoustics Conference] A strict interpretation of that vision would mean no aircraft-related event would produce noise in the community significantly higher than background noise. While this is airport specific, it could easily be argued that present aircraft exceed the vision by 20 to 40 dB. Since presently produced civil transports are already about 20 dB quieter than the earliest jet transports, evolutionary improvements are unlikely to be successful in doubling that achievement.

Turbojet engines were used in the early years of commercial jet service. Much of the reduction in community noise from jetliners since then has come from the use of turbofan engines. Generally, turbofans with higher bypass ratios have lower average exhaust velocity and, consequently, produce less jet noise. Fortunately, engine efficiency normally goes up with bypass ratio, so economics has pushed the trend toward less noisy engines. However, practical limits on engine size have constrained the bypass ratio to about 9, as found on the GE90 turbofan. Also, as jet noise has decreased, noise from the fan and other engine components, as well as from flow over the airframe, has become unmasked, making further noise reduction much more difficult. Thus, a very large reduction in community noise due to an aircraft flyover will probably require an unconventional aircraft design that relies not only on a quiet engine design, but also on propulsion/airframe integration that minimizes noise production and shields the ground from the residual noise.

The EU began investigation of unconventional airframes for achieving large reductions in community noise with the ROSAS project. Results from that effort presented by Ricouard, et al.<sup>1</sup> and Brodersen, et al.<sup>2</sup>, included conventional fuselage and wing configurations with engines placed in unconventional locations. Other investigators have identified and/or developed noise reduction technology for the flying wing or blended-wing-body (BWB) concept, especially as part of NASA's Quiet Aircraft Technology Program<sup>3</sup> and the Silent Aircraft Initiative<sup>4,5,6</sup> funded by the British government and others.

Berton<sup>7</sup> predicted certification levels for a notional, long haul, commercial quadjet transport with advanced ultra-high bypass engines mounted above the wings. Even though he assumed that jet noise and airframe noise were totally unshielded, he calculated reductions in the sideline and cutback levels of more than 4 EPNdB. This was possible because the two largest noise sources from the hypothetical 13.5 bypass ratio engine used in the study were expected to be the fan discharge and the aft-radiating core. Since both these sources were near the center of the wing chord, peak levels below the aircraft were reduced by more than 10 dB for each source. Such sizable attenuations from putting a large engine above the wings of an otherwise conventional configuration airframe suggests that even larger reductions should be possible from more aggressive designs.

In the late 1990s, NASA studied Synergistic Airframe-Propulsion Interaction and Integration (SnAPII) technologies and presented several unconventional aircraft concepts<sup>8</sup> that would use these technologies. The suggested concepts included a forward-swept blended wing body, a Goldschmied blended joined wing, a modified Chaplin V-wing, and variations of a twin-body (catamaran) aircraft. According to that study, each of these concepts has the potential to increase safety, reduce emissions, reduce initial and operational costs, and reduce noise. While aerodynamic efficiency was the prime driver in developing these ideas, many of their characteristics have obvious acoustic advantages: low thrust, high lift at takeoff and approach, and shielding of propulsion noise from ground observers.

The present paper takes a closer look at the noise shielding potential of the catamaran with inboard and outboard wings when coupled with distributed propulsion, a concept based on replacing the conventional two to four engines with a relatively large number of smaller engines. An extreme case of distributed propulsion would be the use of mini-engines (perhaps 10 to 100 lbs. of thrust per engine) placed along the inboard wing and/or inside boundary layer-ingesting inlets at the rear of the twin fuselages. Here, only low-frequency jet noise from mid-wing-mounted engines is considered, because low frequencies are the most difficult to shield. Thus, these calculations put a lower bound on the potential shielding benefit.

## II. □ Distributed Propulsion and the Catamaran Concept

Distributed propulsion is attractive from an acoustic perspective because the wavelengths of most noise from turbofan engines scale linearly with engine size. There are at least two potential advantages associated with shorter wavelengths (higher frequencies): increased atmospheric absorption and improved shielding. Unfortunately, Hill, et al.<sup>9</sup> found in their study of distributed propulsion on a BWB that "...although the higher frequencies [for jet noise] of multiple engines provided an atmospheric absorption benefit, a Perceived Noise Level weighting penalty offset this and the Effective Perceived Noise Levels hardly varied." However, the increase in shielding for higher

frequencies and smaller sources could be large enough to produce significant incentive to pursue distributed propulsion. In fact, Agarwal and Dowling<sup>4</sup> found that the diffracted field from the edge of a wedge drops by 3 dB when the source frequency is doubled, at least in the high-frequency limit. Also, the shorter length of the exhaust jet for smaller engines can bring the jet noise source region above the wing, thus enhancing shielding. This idea is explored further below.

The concept of a twin fuselage aircraft dates at least as far back as 1923 when the Italian firm Savoia-Marchetti built the S-55 (fig. 1). In 1943, the Germans built, but never flew, a prototype of the Messerschmitt Bf 109Z (fig. 2). This consisted of two Bf 109F airframes joined by an inboard wing in order to enhance the range and payload for interceptor and bombing missions. At about the same time, North American designed and built the P-82 Twin Mustang (fig. 3). According to Boeing.com, the P-82 entered service in 1946 and for a while was the “standard long-range, high-altitude escort fighter for the U.S. Air Force.” It also states: “A radical departure from the conventional single-fuselage airplane, the Twin Mustang was formed by two fuselages joined by the wing and the horizontal stabilizer. With a pilot in each fuselage, it reduced to a minimum the problem of pilot fatigue on ultra-long-range missions.”

The catamaran concept was revisited in studies by Spearman<sup>10</sup> during the last decade. He conducted a number of wind tunnel experiments that “...verified the basic concept of the inboard-wing design...” and noted that such a design could have double the payload of a current transport with no increase in length or span. A desktop model of a jumbo cargo catamaran built for Spearman is pictured in figure 4. Note the cockpit projecting forward from the inboard wing between the engines. Obviously, this transport would have a much greater payload than any current aircraft. As discussed by Yaros, et al.<sup>8</sup>, several different wing configurations have been considered for catamaran aircraft, including an inboard wing only, outboard wings with an inboard wing, and two inboard wings in a tandem configuration with one mounted low toward the front and another high toward the rear. All three variants would employ circulation control to maximize lift during terminal area operations and wing morphing to provide better cruise performance.

### III. Noise Source Model

Since shielding is less effective at lower frequencies, a conservative estimate of the potential benefit is obtained by looking near the low end of the frequency range of interest. Also, jet noise is difficult to shield, because it is generated downstream of the engine, normally well downstream of the wing for a wing-mounted engine. Thus, even mounting the engine above the wing would not be expected to provide significant shielding of jet noise unless the engine were much smaller than normal, as in the case of distributed propulsion.

Glegg<sup>11</sup> reviewed jet noise source distribution research. From that presentation, the following assumptions seem to be reasonable and are adopted in the present study. The jet noise spectrum appears to peak near a Strouhal number ( $Str = fD/U_j$ ) equal to unity and drops off sharply below  $Str = 0.25$ . Spatially, the source of  $Str=1$  noise peaks at about five jet diameters downstream of the nozzle exit, and  $Str = 0.25$  near ten diameters.

Because only a rough estimate of frequencies of interest is adequate for the current purpose, the average velocity in the GE-90 nozzle exhaust is assumed to be about 1000 ft/s and the nozzle diameter approximately 8 ft. Thus, the jet spectrum should peak near 125 Hz, with about 30 Hz being the lowest frequency of interest. To reduce calculation time and to be moderately conservative, most calculations presented here are for the part of the spectrum corresponding to 100 Hz in the 2-engine configuration.

Previous studies of distributed propulsion systems by Hill, et al.<sup>9</sup> and Lundbladh<sup>12</sup> conclude that less total thrust is needed for distributed propulsion systems if boundary layer ingestion is added and the engine-out regulation is considered. Here, the conservative assumption is made that total thrust remains constant as the number of engines increases. Furthermore, exhaust nozzle area is taken to be proportional to thrust, so the diameter of each of  $N$  engines is

$$D_N = D_{GE90} (N/2)^{-0.5}.$$

In order to keep the Strouhal number constant, the frequency of interest increases in proportion to the square root of  $N/2$ . For example, if 16 engines are being considered, the portion of the GE90 jet noise spectrum represented by 100 Hz is translated to 283 Hz. As mentioned above, the material presented by Glegg would suggest that this portion of the spectrum has its largest source strength somewhat downstream of 5 nozzle diameters from the exit plane. However, source location measurements presented by Weir, et al.<sup>13</sup> show that noise-reducing chevrons on the nozzle can move source locations significantly upstream. Taking a conservative approach again, the source strength at frequency  $100 (N/2)^{0.5}$  Hz is assumed to peak at 5 diameters.

Jet noise frequencies could be raised even further and the source region made more compact if distributed exhaust nozzles<sup>14,15</sup> (DENs) were used on the small engines. A DEN breaks the exhaust flow from an engine into

many smaller jets, ideally greatly increasing frequencies and moving the sound-producing region closer to the nozzle exit plane. The cited studies tested several DEN designs and found good acoustical performance along with large engine performance penalties. The performance penalties would be acceptable if there were a very large premium on quiet terminal area operations and the DEN could be disabled during cruise. Again, trying to arrive at a conservative estimate of shielding benefits, the use of DENs is not assumed in the calculations that follow.

#### IV. □Noise Scattering Model

In this study, many simplifying assumptions are used to facilitate relevant calculations without the cost and time associated with more precise, multi-disciplinary system studies. In essence, the present work might be considered a proof-of-concept study from an acoustical perspective. In that spirit, an existing grid for a large twin-engine transport powered by two GE90 engines was taken as a starting point. A twin fuselage configuration was created with two bodies joined by an inboard wing with a chord equal to 21% of the fuselage length and a span of 33% of the length. The new configuration was sized such that the twin fuselages have a combined volume equal to that of the single original fuselage. That is, the original linear dimensions are divided by the cube root of 2 so that each of the twin fuselages has half the volume of the original. The resulting aircraft geometry is shown in figure 5 with a total length of 163.6 ft and an inboard wing with a 34.1 ft chord and 54.0 ft span.

Shielding concepts for the above catamaran configuration and derivatives are studied using the Fast Scattering Code (FSC)<sup>16</sup>. The frequency domain FSC is chosen for this research because three-dimensional aeroacoustic scattering predictions in the frequency range under consideration can be obtained with 2006 computer workstation technology. To employ the FSC for this purpose, jet noise radiation is modelled by simple point monopoles and dipoles placed above the inboard wing of the catamaran at locations aft of the proposed distributed propulsion jet nozzles. In the interest of simplicity, symmetric scattering geometry and noise source placement were employed. For advanced analyses of jet noise scattering using the FSC, researchers might incorporate more sophisticated combinations of multipoles to better simulate jet noise characteristics or input incident sound from some jet noise radiation code.

The FSC is a computer program designed to predict the three-dimensional scattered acoustic field produced by the interaction of known, time-harmonic, incident sound with aerodynamic structures of arbitrary shape in the presence of a known, low speed, potential background flow. Governing acoustic differential equations for the FSC are obtained from a small perturbation analysis of the inviscid flow equations. The resulting exterior boundary value problem for the unknown acoustic pressure and velocity is given in equations 1-4. In equation (3), scattering surfaces can be acoustically hard or sound absorbant<sup>17</sup> in which case the user specifies local surface admittance. To solve the BVP, the acoustic variables are split into known incident and unknown scattered parts. The incident portion of the field satisfies equations (1), (2), and (4) and provides the inhomogeneous source terms in the boundary condition (3). Details of the derivations, FSC solution methodology, applications, and validation with experimental data can be found in references 18-20.

Mass conservation:

$$ik_0 p' + \rho_0 c_0 \nabla \cdot \left( \frac{p'}{\rho_0 c_0} \vec{M}_0 + \vec{v}' \right) = 0 \quad \vec{x} \in S^+ \quad (1)$$

Momentum conservation:

$$ik_0 \vec{v}' + \frac{1}{\rho_0 c_0} \nabla (p' + \rho_0 c_0 \vec{M}_0 \cdot \vec{v}') = 0 \quad \vec{x} \in S^+ \quad (2)$$

Boundary condition:

$$\vec{v}' \cdot \hat{n} = Ap' \left[ \frac{1}{ic_0 k_0} \hat{n} \cdot (\hat{n} \cdot \nabla c_0 \vec{M}_0) - 1 \right] - \left( \frac{1}{ik_0} \vec{M}_0 \cdot \nabla Ap' \right) \vec{M}_0 \quad \vec{x} \in S \quad (3)$$

Radiation condition:

$$\lim_{R \rightarrow \infty} \left[ R \left( \frac{\partial p'}{\partial R} + i \kappa_o p' \right) \right] = 0 \quad (4)$$

In the simulations that follow, the FSC is used to quantify shielding in the aft portions of both the near and far fields. The effects of atmospheric absorption on farfield radiation are neglected. Nearfield calculations from the FSC could be used as input into more physically correct farfield radiation codes to account for atmospheric effects. Also, to avoid complications associated with generating realistic flows for the catamaran geometries, the uniform flow option of the FSC was used.

Sample noise scattering calculations for the above catamaran configuration at  $M = 0.3$  are shown in figure 6 for a frequency of 203 Hz. Incident sound representative of that produced by the jet of one engine is generated by two point monopoles separated by one-half wavelength and situated mid-span above the inboard wing. Contours of noise shielding (incident minus total) are plotted on both the upper and lower aircraft surfaces. As expected, significant shielding is observed on the fuselage walls adjacent to the outer wings and beneath the inboard wing.

Computer memory limitations with available resources prevents higher frequency predictions with this configuration. FSC requires memory proportional to  $Sf^2$ , where  $S$  = area of scattering surfaces and  $f$  = excitation frequency. To increase the computational frequency range, two reduced-area catamaran geometries were constructed. A derivative of the figure 5 aircraft is obtained by shortening the forward portions of the fuselages. Noise predictions on the surface of this configuration are shown in figure 7. Shielding trends on the aft portion of the aircraft show little effect of the shortened fuselages (compare with figure 6). A third geometry features a wider inboard wing with outer wings removed. Figure 8 shows that this geometry also produces aft shielding patterns similar to the original. The reduced area derivatives increase the maximum frequency achievable with available resources by 50%, facilitating parametric noise studies presented in the next section.

## V. □ Results

Two noise source configurations are considered. In each case, the source location along the wing chord is appropriate for about 12 to 16 engines. First, one engine above the middle of the inboard wing is modeled by two monopoles situated one-half wavelength apart so as to produce a source directivity similar to that of jet noise in the lateral direction. This source system is applied to the two derivative geometries and is used to study the effect of inboard wing chord length on near and far field shielding. Also, the effects of treating the trailing edge portion of the inboard wing with an acoustic liner is examined. Secondly, to study the shielding properties of a full 12-engine distributed propulsion system, jet noise radiation is simulated by a spanwise array of 12 monopoles (or axial dipoles) located midchord above the inboard wing of the wide inboard wing geometry.

In figure 9, the farfield shielding benefits of increasing the chord of the inboard wing are examined. With the aircraft at an altitude of 2000 ft, field plots of shielding vs. distance along the ground aft of the noise source are presented for four sideline angles (0, 10, 20, and 30 degrees) for both the wide inboard wing and extended fuselage configurations. The zero degree sideline angle corresponds to locations directly under the aircraft path. Note that the successive patterns of cancellation and reinforcement evident in these results do not appear in the incident sound and must be attributable to the complexities induced by the scattering surfaces. The installation of a wider inboard wing not only increases the amount of shielding under the aircraft, but also extends downstream the region in which shielding occurs.

Further noise reduction is achievable by adding regions of sound absorption on the inboard wing. To illustrate this feature, a locally reacting liner model with constant impedance ( $Z = \rho c(1.0 + 0.5i)$ ) was applied to the wing trailing edge of the wide inboard wing configuration. Figure 10 displays contours of noise reduction ( $SPL_{HW}$  minus  $SPL_{LINER}$ ) on the aircraft surfaces. Calculations show that the liner accounts for up to 4-5dB reduction on the bottom/inner portion of the catamaran fuselages aft of the wing. Farfield calculations showed little difference in shielding between lined and unlined configurations. This sample liner calculation was chosen for its ease of implementation. No effort was expended to determine optimal impedance values or improved liner locations. It is suggested that incorporating liner optimization concepts to the scattering surfaces near the incident sources should provide additional noise reduction at least on the fuselage areas.

The calculations above are meant to represent minimum shielding by including only the noise from a single jet located at center span on the inboard wing. Calculations for a full 12-engine configuration are given in figures 11

and 12. Each jet is represented by a dipole to produce a directional source. For computational efficiency, symmetrically placed sources are coherent, but each pair is incoherent with respect to the other pairs. Figure 11 shows the incident field and total field in the source plane. Excellent shielding is evident, as expected. Farfield shielding is shown in figure 12 on a plane 2000 ft below the aircraft. Summing several uncorrelated sources eliminates most of the extreme peaks and valleys in the sideline plots, giving shielding for the frequencies and ranges shown the order of 10 dB. Remembering that these frequencies are at the low end of jet noise and much lower than most fan or core noise, total engine noise shielding would be greater. If the 3 dB increase in shielding for each doubling of frequency previously mentioned is applicable, fan blade passage frequencies in the neighborhood of 2 kHz would be reduced by about 20 dB over a very large area. More engines could be fit onto the inboard wing by clever imbedding/distribution schemes, increasing frequencies even more and bringing the exhaust jets closer to the wing, leading to even better shielding.

## VI. □ Conclusions

In this proof-of-concept study, simple low-frequency jet noise source and 3-D scattering models were used to demonstrate the noise shielding potential of a catamaran type aircraft. Calculations suggest that acoustic shielding provided by a catamaran aircraft with distributed propulsion could reduce community noise from the propulsion system by more than 20 dB over large areas. Nearfield predictions indicate that the aft/outboard quadrants of the fuselages show significant shielding due to the proposed geometry and source configuration. The aft/inboard fuselage quadrants receive direct radiation from the sources, but simple liner calculations indicate the possibility of >5 dB noise reduction in that area by liner treatment beneath the sources on the inboard wing. Predictions for this catamaran configuration at frequencies greater than 320 Hz require larger memory computers than those used here.

The jet noise source and scattering models presented here were simplified for computational expediency. 3-D noise predictions with the Fast Scattering Code, using 2006 workstation technology, were conducted for various catamaran configurations and low-frequency jet noise source distributions. At increased computational cost, the FSC has capabilities for advanced source and propagation modeling. For example, the FSC has options for including inviscid flow effects, importing incident sound from advanced jet noise radiation codes, and providing nearfield input for external atmospheric propagation codes. These features, when combined with larger memory computers, increase the range of applicability of the FSC to assess shielding characteristics of advanced configurations such as the catamaran design.

## Acknowledgments

This work was sponsored by NASA's Fundamental Aerodynamics Research Program.

## References

- <sup>1</sup>Ricouard, J., Davy, R., Loheac, P., Moore, A., Piccin, O., "ROSAS Wind Tunnel Test Campaign Dedicated to Unconventional Aircraft Concepts Study," AIAA-2004-2867, May, 2004.
- <sup>2</sup>Brodersen, O., Taupin, K., Maury, E., Spieweg, R., Lieser, J., Laban, M., Godard, J., Vitagliano, P., and Bigot, P., "Aerodynamic Investigations in the European Project ROSAS (Research on Silent Aircraft Concepts)," AIAA-2005-4891, June, 2005.
- <sup>3</sup>Hill, G. A. and Thomas, R. H., "Challenges and Opportunities for Noise Reduction Through Advanced Aircraft Propulsion Airframe Integration and Configurations," 8<sup>th</sup> CEAS-ASC Workshop: Aeroacoustics of New Aircraft and Engine Configurations, Budapest, Hungary, 2004. (archived at [http://www.win.tue.nl/ceas-asc/workshop8/CEAS\\_8\\_programme.html](http://www.win.tue.nl/ceas-asc/workshop8/CEAS_8_programme.html))
- <sup>4</sup>Agarwal, A., and Dowling, A. P., "The calculation of Acoustic Shielding of Engine Noise by the Silent Aircraft Airframe," AIAA paper 2005-2996, May, 2005.
- <sup>5</sup>Hall, C. A., and Crichton, D., "Engine and Installation Configurations for a Silent Aircraft," AIAA 2004-0854, 2004.
- <sup>6</sup>Manneville, A., Pilczner, D., and Spakovszky, Z. S., "Noise Reduction Assessments and Preliminary Design Implications for a Functionally-Silent Aircraft," AIAA paper 2004-2925, May 2004.
- <sup>7</sup>Berton, J. J., "Noise Reduction Potential of Large, Over-the-Wing Mounted, Advanced Turbofan Engines," NASA/TM-2000-210025, April 2000.

- <sup>8</sup>Yaros, S. F., Sexstone, M. G., Huebner, L. D., Lamar, J. E., McKinley, R. E., Torres, A. O., Burley, C. L., Scott, R. C., and Small, W. J., "Synergistic Airframe-Propulsion Interactions and Integrations," NASA TM-1998-207644, NASA Langley Research Center, Hampton, VA, 1998.
- <sup>9</sup>Hill, G. A., Brown, S. A., Geiselhart, K. A., and Burg, C. M., "Integration of Propulsion-Airframe-Aeroacoustic Technologies and Design Concepts for a Quiet Blended Wing-Body Transport," AIAA paper 2004-6403, September 2004.
- <sup>10</sup>Spearman, M. L., "An Airplane Design having a Wing with a Fuselage Attached to Each Tip," AIAA paper 2001-0536, January 2001.
- <sup>11</sup>Glegg, S. A. L., "Jet Noise Source Location: A Review", in Proceedings of the Jet Noise Workshop, NASA/CP-2001-211152, p. 439-478, September 2001.
- <sup>12</sup>Lundbladh, A., "Distributed Propulsion And Turbofan Scale Effects," paper ISABE-2005-1122, 17<sup>th</sup> International Symposium on Airbreathing Engines, Munich, Germany, September 2005.
- <sup>13</sup>Weir, D., Bridges, J., and Agbooli, F., "Honeywell Engines and Systems Engine Validation of Noise Reduction Concepts," NASA/CP-2001-211152, p. 483-506, September 2001.
- <sup>14</sup>Kinzie, K. W., Schein, D. B., and Solomon, D., "Experiments and Analyses of Distributed Exhaust Nozzles," AIAA Journal, vol.43, no.7, pp.1476-1481, 2005.
- <sup>15</sup>Gaeta, R., Ahuja, K., Murdock, B., and Combier, R., "Noise Reduction from a Distributed Exhaust Nozzle with Forward Velocity Effects," AIAA-2004-2970, May 2004.
- <sup>16</sup>Tinetti, A. F., Dunn, M. H., and Pope, D. S., Fast Scattering Code (FSC) User's Manual, Version 2.0, January 30, 2006.
- <sup>17</sup>Myers, M.K., "Acoustic generation by vibrating bodies in homentropic flow at low Mach number," *Journal of Sound and Vibration*, Vol. 65, pp. 125-136, 1979.
- <sup>18</sup>Dunn, M. H. and Tinetti, A. F., "Aeroacoustic Scattering via the Equivalent Source Method," AIAA paper 2004-2937, May 2004.
- <sup>19</sup>Tinetti, A.F. and Dunn, M.H., "Aeroacoustic noise prediction using the Fast Scattering Code", AIAA 2005-3061, May 2005.
- <sup>20</sup>Gerhold, C.H., Clark, L.R., Dunn, M.H., and Tweed, J., "Investigation of acoustical shielding by a wedge-shaped airframe", Accepted for publication by *Journal of Sound and Vibration*, October, 2005.

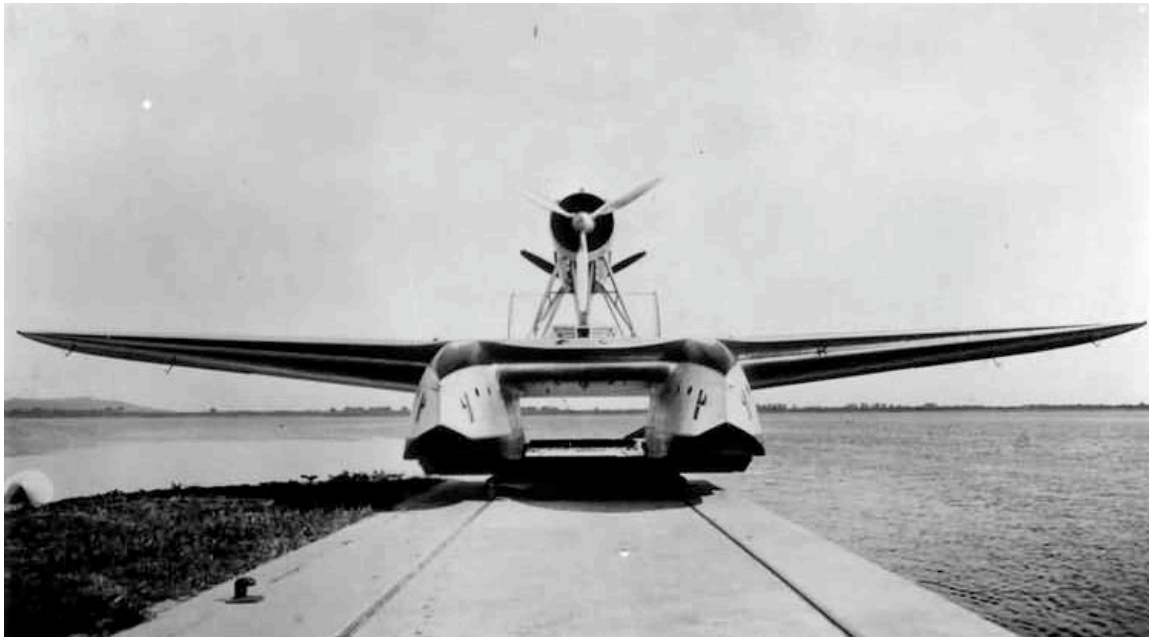


Figure 1. Savoia-Marchetti S-55. Early catamaran aircraft built in 1923.

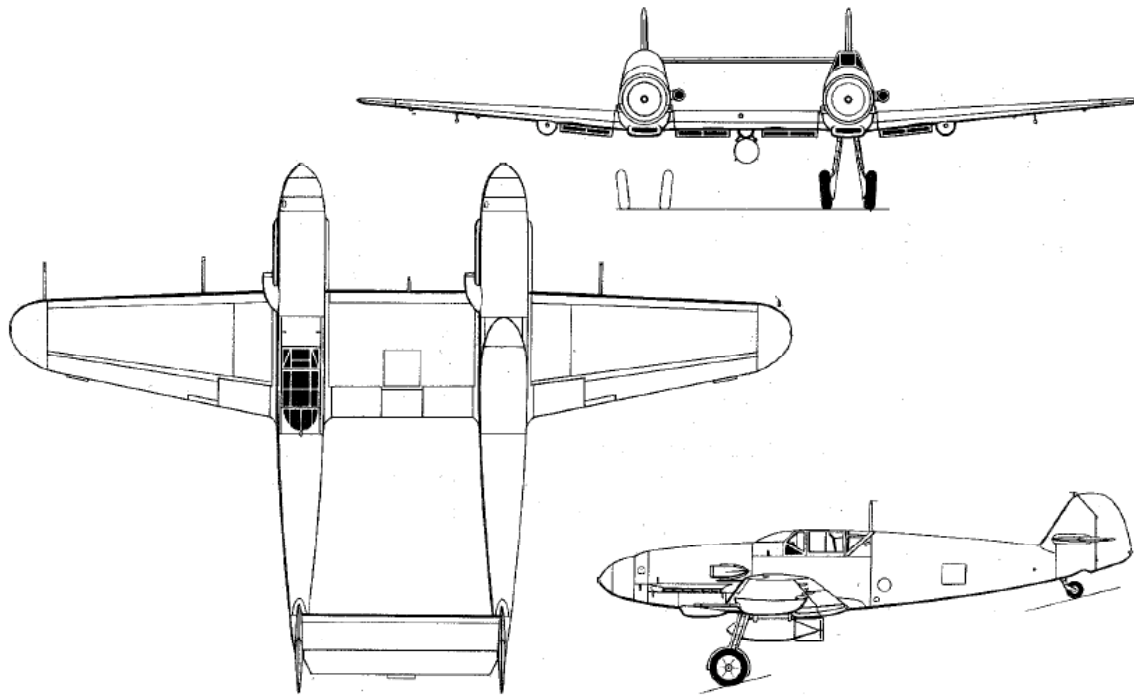


Figure 2. Messerschmitt Bf109Z. Prototype built in 1943, but it never went into production.



Figure 3. P-82 entered service in 1946. North American built 274 aircraft. This is a picture of a powered model with a five foot wing span.





Figure 4. Model of very large catamaran aircraft studied by NASA. Note the cockpit between the two center engines.

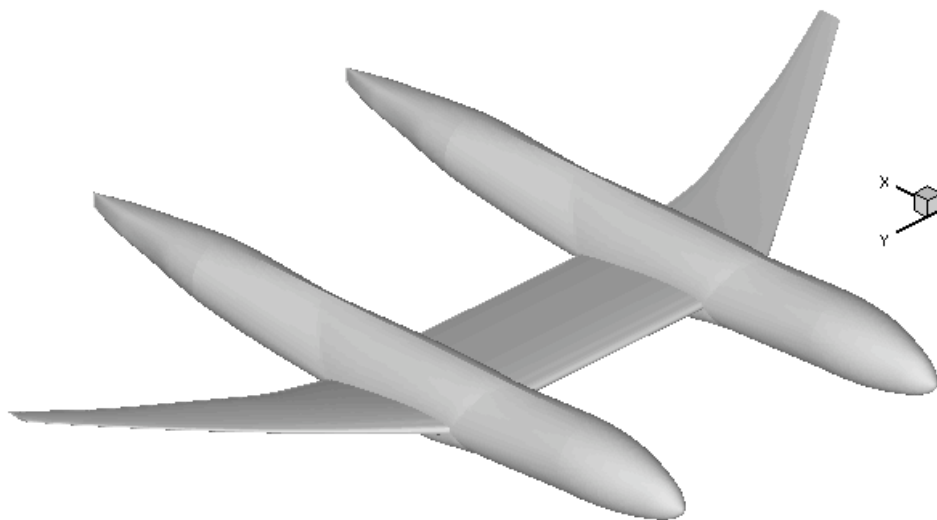


Figure 5: Computational model of conceptual catamaran transport

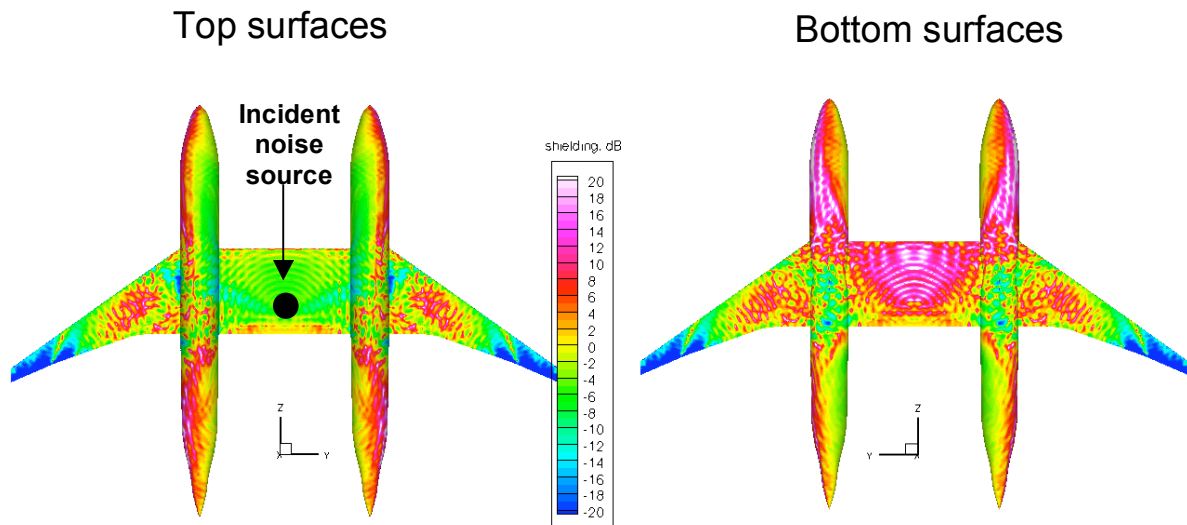


Figure 6: Shielding contours on surfaces of original catamaran aircraft  
 $f = 203 \text{ Hz}$ ,  $M = 0.3$

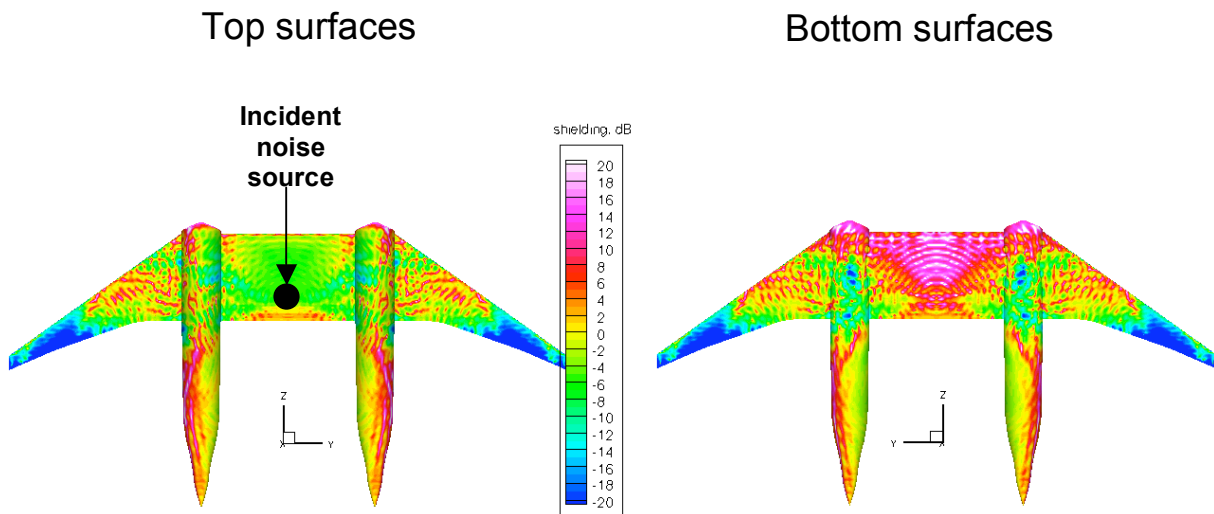


Figure 7: Shielding contours on surface of fuselage shortened catamaran aircraft  
 $f = 203 \text{ Hz}$ ,  $M = 0.3$   
 Incident noise generated by two monopoles above wing,  $0.5\lambda$  apart

Top surfaces

Bottom surfaces

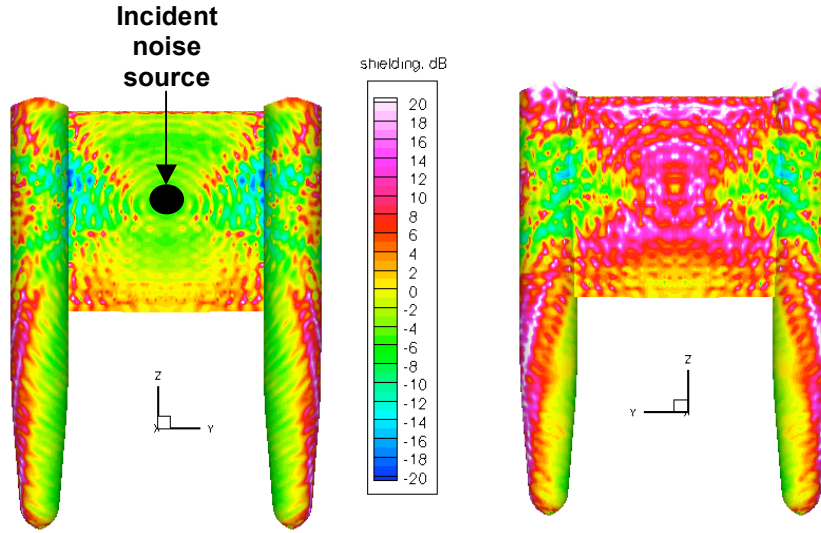


Figure 8: Shielding contours on surface of wide inboard wing catamaran aircraft

Shortened fuselage configuration

Wide inboard wing configuration

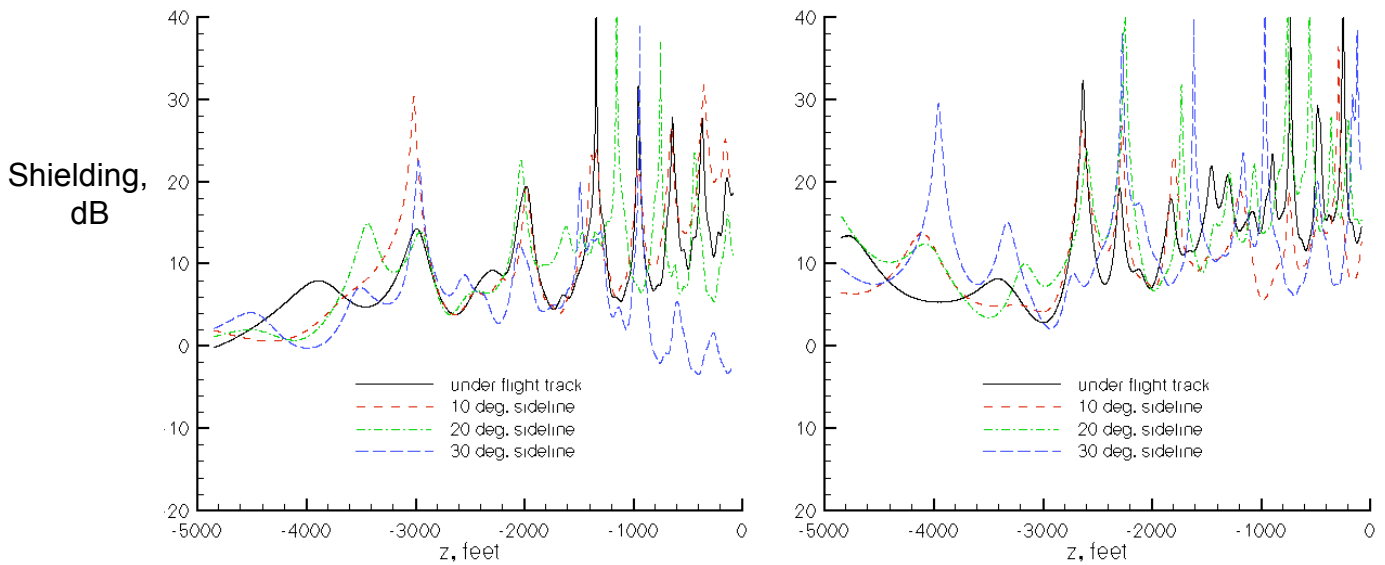


Figure 9: Far field shielding at four sideline locations 2000 ft below aircraft  
 $f = 316 \text{ Hz}$ ,  $M = 0.3$   
 Incident noise generated by two monopoles above wing,  $0.5\lambda$  apart

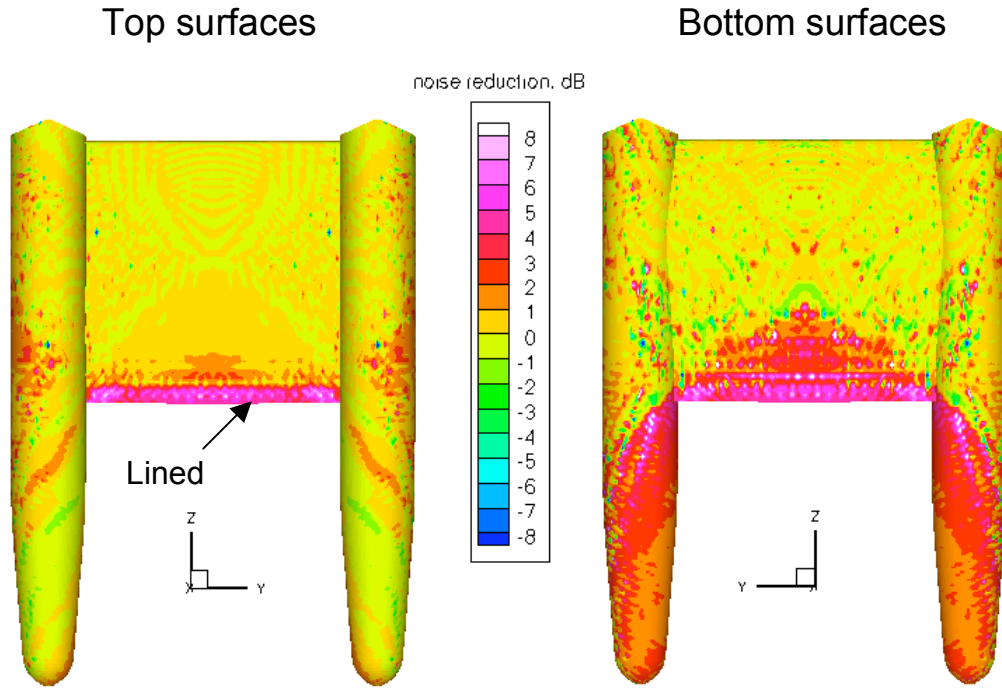


Figure 10: Noise reduction contours ( $SPL_{HW}$  minus  $SPL_{LINER}$ ) due to acoustic liner at inboard wing trailing edge  
 $f = 316 \text{ Hz}$ ,  $M = 0.3$ ,  $Z = \rho c(1.0+1.5i)$   
 Incident noise generated by two monopoles above wing,  $0.5\lambda$  apart

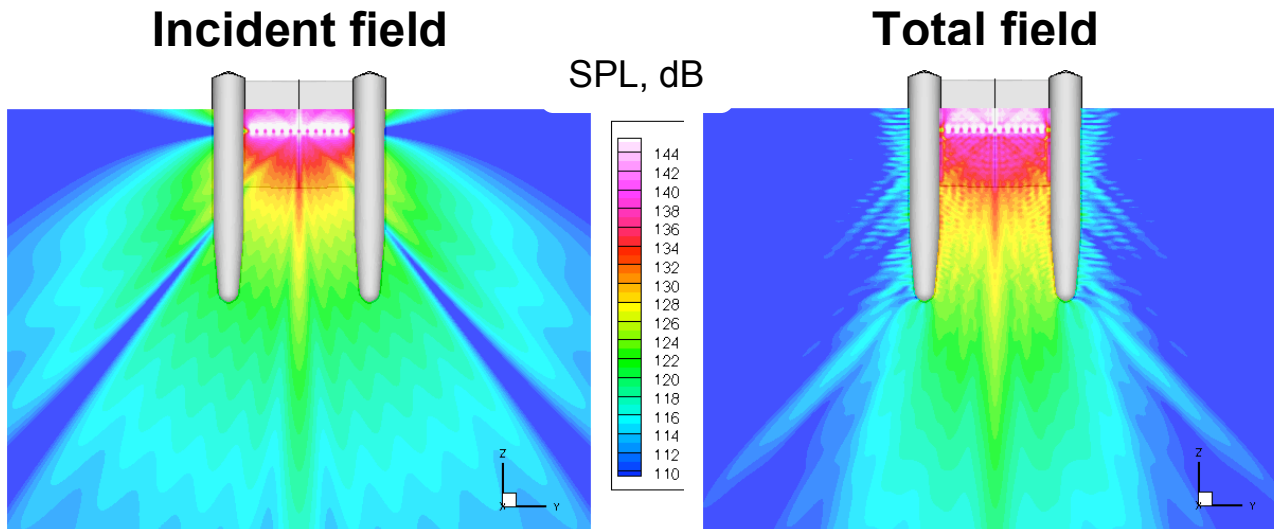


Figure 11. Incident and total sound fields (in the source plane) for twelve evenly spaced dipoles along the inboard wing at the chord location appropriate for peak jet noise from twelve engines with total power equal to that of 2 GE90-85 engines.  $f = 203 \text{ Hz}$ ,  $M = 0.3$

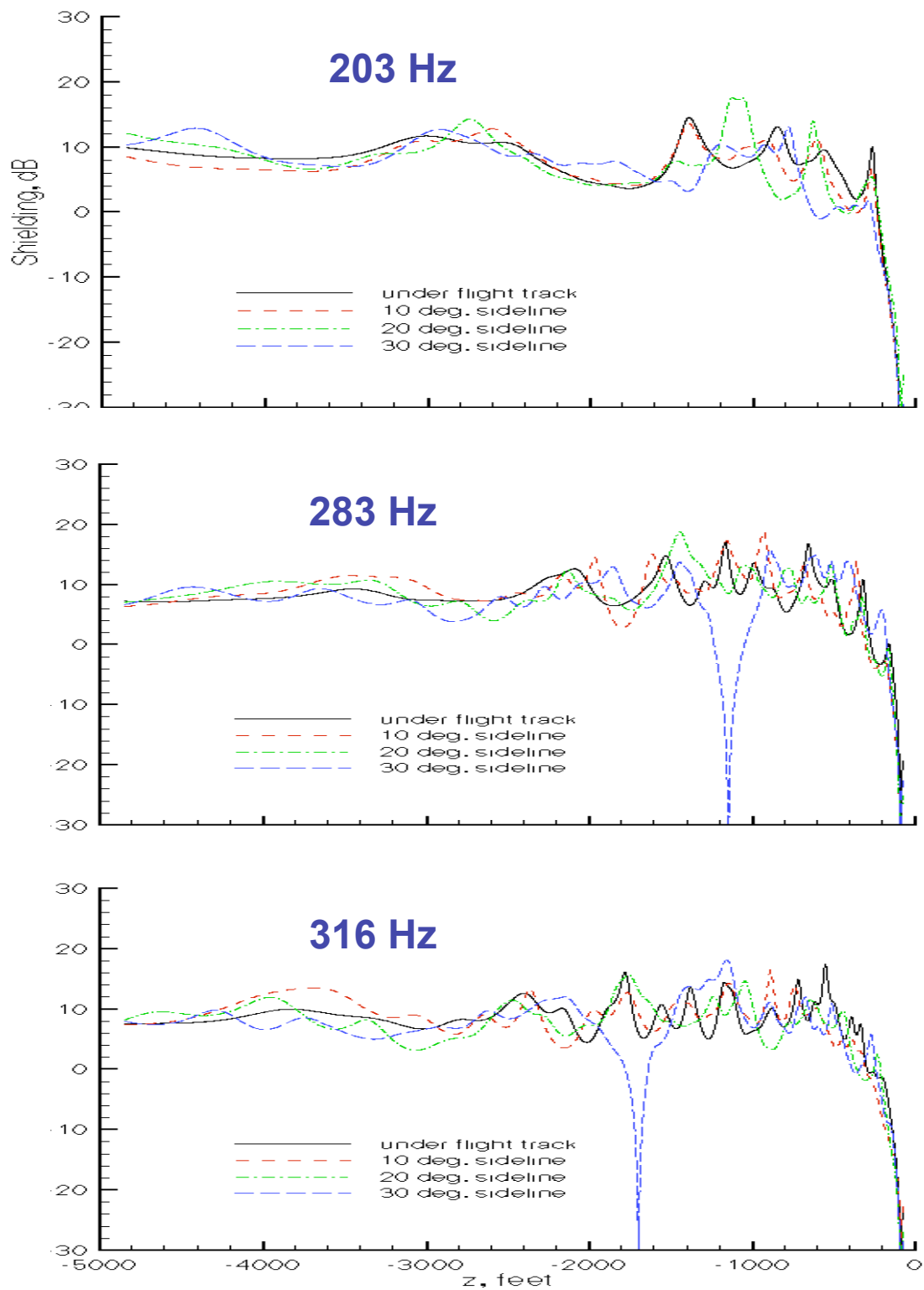


Figure 12. Far field shielding at four sideline locations 2000 ft below aircraft  
 $f$  as shown for each chart,  $M = 0.3$   
 Incident noise generated by 12 dipoles above wide-chord wing